This is the Pre-Published Version.

This is the Accepted Manuscript version of an article accepted for publication in Journal of The Electrochemical Society. IOP Publishing Ltd is not responsible for any errors or omissions in this version of the manuscript or any version derived from it. The Version of Record is available online at https://doi.org/10.1149/2.0041611jes.

This manuscript version is made available under the CC-BY-NC-ND 4.0 license (https://creativecommons.org/licenses/by-nc-nd/4.0/)

Modeling of Direct Carbon-Assisted Solid Oxide Electrolysis Cell for Syngas Production at Two Different Electrodes

Haoran Xu, Bin Chen*, Meng Ni

Building Energy Research Group, Department of Building and Real Estate, The Hong Kong Polytechnic University, Hung Hom, Kowloon, Hong Kong

Abstract:

H_2O/CO_2 co-electrolysis by fuel-assisted solid oxide electrolyzer cell (SOFEC) could greatly reduce power consumption for syngas production. H_2 and CO are both produced in the cathode and the gas composition is difficult to control. In this paper, direct carbon assisted SOEC for H_2O electrolysis (DC-SOFEC) is proposed for syngas production with easy control of H_2/CO ratio. A 2D numerical model is developed to study the effects of operating and design parameters on the DC-SOFEC performance. The model is validated with experimental data for direct carbon solid oxide fuel cell. One important finding is that the carbon assisting is effective in lowering the equilibrium potential of SOEC, thus greatly reduces the electrical power consumption for H_2O electrolysis. The DC-SOFEC can generate electrical power, CO and H_2 simultaneously at a low current density and sufficiently high temperature. Compared with conventional SOEC for H_2O/CO_2 co-electrolysis, DC-SOFEC is advantageous as CO and H_2 are produced in the anode and cathode, respectively. This enables easy control of H_2/CO ratio, which is helpful for subsequent processes to synthesis other chemicals or fuels from syngas. The model can be used for subsequent design optimization of SOFEC for effective energy storage and conversion.

Keywords: Solid oxide electrolyzer cell (SOEC); Mathematical modeling; Electricity and syngas cogeneration; Solid oxide fuel cell; Carbon

* Corresponding author:
Email: chenbinxjtu@gmail.com (Bin CHEN), Tel: 852 – 34008126

1. Introduction

Clean and sustainable energy technologies are urgently needed to address the fossil fuels-related energy crisis and environmental problems such as global warming, air pollution and acid rain. Renewable energies such as solar energy and wind energy, can hopefully meet our requirements. However, they are discrete in time and space, thus not reliable for continuous energy supply. Therefore, effective energy storage is critical for renewable energy applications to mitigate the mismatch between energy supply and demand. Moreover, the development of smart grip also needs effective energy storage to ensure reliable and efficient power supply.

Solid oxide electrolysis cell (SOEC), a high temperature electrochemical cell, is suitable for converting excessive renewable power to fuels. The produced fuel can be stored and converted back into electrical power via fuel cells when the renewable power is insufficient. Compared with low temperature electrolyzers, the electricity requirement of SOEC is relatively lower as a significant part of total energy needed for SOEC is in the form of heat. In addition, the high operating temperature of SOEC enables the use of non-noble metal catalyst, leading to lower cost than low temperature electrolyzer systems. SOECs are capable of co-electrolyzing CO_2 and H_2O to produce syngas (H_2 and CO mixture), which can be further processed to gaseous or liquid fuels using Fischer-Tropsch (F-T) reactor. This offers an alternative way of utilizing the captured CO_2 for fuel synthesis using excessive renewable power.

For practical application of SOEC, its electricity consumption needs to be further reduced as the quality of electricity (i.e. exergy) is high. Recent studies have demonstrated that by supplying low cost fuel (such as CH_4 and CO) to the anode of SOEC (termed as fuel-assisted SOEC: SOFEC) for steam electrolysis could significantly reduce the operating potential of SOEC, thus greatly reduce the electrical power consumption[1-4]. Compared CH_4 and CO, the use of carbon for assisting SOECs can significantly reduce the system cost. Gopalan et al.[5] proposed and developed a coal-based solid oxide fuel cell for hydrogen generation using metal Ag as electrode. Ewan et al.[6] developed and analyzed carbon assisted electrolysis cell, developed from direct carbon fuel cell, finding that carbon char is very suitable as an assisting fuel for the current solid oxide electrolysis cell technologies. Gür and Liu et al. demonstrated and proposed gasification-driven direct carbon fuel cell, termed as GD-DCFC or DC-SOFC[7-13]. The GD-DCFC is a whole-solid state device without any liquid media, thus avoiding liquid corrosion and leakage problems. At the same time, CO participates in the electrochemical reactions in GD-DCFC, in which the TPB sites is much more than that of solid carbon so that the oxidation rate of solid carbon is enhanced by means of Boudouard reaction.

Based on the concept of GD-DCFC, a 2D mathematical model is developed for an axisymmetric-tubular direct carbon assisted solid oxide electrolysis cell (DC-SOFEC) for H_2O electrolysis and syngas production. The model is validated with experimental data for electrolyte-supported direct carbon solid oxide fuel cell and can be applied for further study. Parametric simulations are conducted to understand the effect of carbon

assisting on the performance of SOEC and the interplay of different physical/chemical processes.

2. Model development

2.1. Model assumptions and Geometries

Numerical model of tubular DC-SOFEC is developed by coupling governing equations of electrochemical reactions, chemical reactions, ion/electronic charge transport, mass transport and momentum transport. As Liu et al.'s experimental work[13] on DC-SOFC provides detailed information on operating conditions and cell parameters, their cell configuration is adopted for the present numerical modeling. Due to the excellent reversible operating characteristic of fuel cell, the electrochemical properties of the cell in the fuel cell mode are adopted for the electrolysis mode.

The schematic of the tubular DC-SOFEC unit is shown in Fig. 1. One end of the anode chamber is sealed. Activated carbon powder (Aladdin, 8-16 mesh) is supplied to anode chamber and water vaper is supplied to the cathode channel. The carbon powder reacts with O_2 in anode chamber to form CO_2, which further react with carbon through Boudouard reaction to produce CO. The CO gas is then diffused to the triple phase boundary (TPB) in the porous anode to reacts with O^{2-} form CO_2. Subsequently, the electrochemically produced CO_2 diffuses back to anode chamber to react with carbon to form CO. This reaction route repeats between anode chamber and anode electrode, with net CO production and electricity generation as shown in Eqs (1, 3-5).

The cell in the present study has a length of 9cm (L_{cell}), an inner diameter of 11.5mm and an outer diameter of 12.0mm. The thickness of anode, electrolyte and cathode are 20μm, 201μm and 20μm, respectively. In addition, the tubular SOFEC uses Ag-GDC (the mixture of silver and gadolinium doped ceria, $Ce_{0.8}Gd_{0.2}O_{1.9}$) for both anode and cathode, and YSZ (yttrium stabilized zirconium) for electrolyte. The materials of both electrodes are porous enough for gas transport and the electrolyte is dense enough to separate gases of anode and cathode. The current is measured at operating voltage ranging from 0.7 V to -0.1 V, where positive voltage means the cell generates electricity and negative means the cell consumes electricity.

The main assumptions are listed as following:

(1) The electrochemical reactions spatially occur along electrode thickness within the porous electrodes. The active sites for electrochemical reactions are assumed to be uniformly distributed in the porous electrodes. The two conducting phases (electronic and ionic) are considered to be homogeneous in the porous electrodes.

(2) The ionic and electronic charge transport processes take place in PEN (Positive Electrode-Electrolyte-Negative electrode assembly). The charge transfer reactions are assumed to take place all through the porous electrodes at TPB.

(3) All of the gases (CO, CO_2, H_2 and H_2O) are considered as ideal gases. The flow is considered to be incompressible.

(4) Temperature distribution is uniform in DC-SOFEC.

(5) The volume of activated carbon in anode chamber does not change.

2.2. Governing equations

The micro-scale tubular DC-SOFEC model couples the process of electrochemical reactions in porous electrodes, chemical reactions in chamber, ion/electronic charge transport in electrolyte and electrodes, mass&momentum transport in channels and electrodes.

2.2.1. Chemical reaction model

In the anode side, reversed Boudouard reaction is considered as the governing reaction at the solid carbon-gas phase interface, as shown in Eq. (1).

$$C + CO_2 = 2CO \quad (1)$$

where the initial CO_2 comes from the reaction between carbon and initial O_2 in anode. When DC-SOFEC starts to operate, CO_2 can be electrochemically produced. The reversed Boudouard reaction rate is calculated by Eq. (2)[14]:

$$R_{rb} = k_{rb}\exp(-E_{rb}/RT)c_{CO_2} \quad (2)$$

2.2.2. Electrochemical reaction model

As shown in Fig.1, the CO/CO_2 gas mixture and H_2O/H_2 mixture are at the anode and cathode, respectively. . In the porous cathode, H_2O molecule diffuses through the porous electrode to the triple-phase-boundary (TPB) in the whole cathode, where it is reduced to oxygen ions (O^{2-}) and H_2 via reactions (3).

$$H_2O + 2e^- \rightarrow H_2 + O^{2-} \quad (3)$$

The oxygen ions transport through the dense electrolyte to TPB at anode, where they lose electrons and form CO_2 molecules with CO as described in reaction (4).

$$CO + O^{2-} \rightarrow CO_2 + 2e^- \quad (4)$$

The overall electrochemical reaction can be written as:

$$CO + H_2O \rightarrow CO_2 + H_2 \quad (5)$$

In operation, the required potential (V) applied to SOEC can be expressed as:

$$V = E + \eta_{act,an} + \eta_{act,ca} + \eta_{ohmic} \quad (6)$$

where E is the equilibrium potential (Nernst potential) related with thermodynamics; η_{act} is the activation overpotentials reflecting the electrochemical activity of the electrodes; η_{ohmic} is the ohmic overpotential influenced by ionic and electronic conduction. It should be noted that the concentration overpotentials are not included in Eq. (6) as the gas partial pressure at the reaction sites (TPB) are used in the calculation of equilibrium potential.

2.2.2.1. Equilibrium potential (Nernst potential)

In DC-SOFEC, the equilibrium potentials for reactions (5) can be separated to two parts of partial equilibrium potential in cathode and anode as shown in Eqs. (7) - (8).

$$E_{H_2-H_2O,ca} = \frac{RT}{2F}\ln(\frac{P^L_{H_2O,ca}}{P^L_{H_2,ca}}) \quad (7)$$

$$E_{CO-CO2,an} = \frac{RT}{2F}\ln(\frac{P^L_{CO_2,an}}{P^L_{CO,an}}) \quad (8)$$

where R is the universal gas constant (8.3145 J $mol^{-1}K^{-1}$); T is temperature (K); F is the Faraday constant (96485 C mol^{-1}) and P^L_{CO}, $P^L_{CO_2}$, $P^L_{H_2}$ and $P^L_{H_2O}$ are the local partial pressures of CO, CO_2 ,H_2 and H_2O at the TPB (reaction sites), respectively. The overall Nernst potential in DC-SOFEC is the difference of cathode and anode partial equilibrium potential.

2.2.2.2. Activation overpotential

The activation overpotentials are related to the activation energy barriers for electrochemical reactions to proceed. The Butler-Volmer equation is widely used for determining the relationship between the activation overpotential and the current density:

$$i = i_0\left\{\exp\left(\frac{\alpha nF\eta_{act}}{RT}\right) - \exp\left(\frac{(1-\alpha)nF\eta_{act}}{RT}\right)\right\} \quad (9)$$

where i_0 is the exchange current density, α is the electronic transfer coefficient and n is the number of electrons transferred per electrochemical reaction.

2.2.2.3. Ohmic overpotential

The ohmic overpotential in a SOFEC consists of ionic ohmic overpotential and electronic ohmic overpotential. The ionic and electronic conductivity of electrode and electrolyte materials can be found in Table. 1. The ohmic overpotential can be calculated by the Ohm's law:

$$i_l = -\sigma_l{}^{eff}\nabla(\emptyset_l) \quad (10)$$

$$i_s = -\sigma_{s.eff}\nabla(\emptyset_s) \quad (11)$$

Where $\sigma_{l.eff}$ and $\sigma_{s.eff}$ are the effective ionic and electronic conductivity, $\emptyset_l$ and $\emptyset_s$ are the ion conducting and electron conducting electric potentials, respectively. In porous electrodes, they are related with the structure parameters including volume fraction and tortuosity as:

$$\sigma_l{}^{eff} = \sigma_l \cdot \frac{V_l}{\tau_l} \quad (12)$$

$$\sigma_s{}^{eff} = \sigma_s \cdot \frac{V_s}{\tau_s} \quad (13)$$

where σ_l and σ_s are the intrinsic ionic and electronic conductivity as listed in Table 1.

2.2.3. Mass transport model

In the porous electrode, gas diffusion occurs by means of both free molecular diffusion and Knudsen diffusion. Free molecular diffusion dominates in large pores and Knudsen diffusion becomes significant when pore sizes are comparable or smaller than molecular mean-free path. The extended Fick's model is used to describe gas transport in the porous electrodes as:

$$N_i = -\frac{1}{RT}\left(\frac{B_0 y_i P}{\mu}\frac{\partial \mathrm{P}}{\partial \mathrm{z}} - D_i^{eff}\frac{\partial(y_i \mathrm{P})}{\partial \mathrm{z}}\right) \quad (i = 1, \dots, n) \quad (14)$$

Where N_i represents the flux of mass transport, B_0 is the permeability coefficient, y_i is the mole fraction of component i, μ is the dynamic viscosity of the gas and D_i^{eff} is the effective diffusivity of species i. In an SOEC where both molecular diffusion (D_{im}^{eff}) and Knudsen diffusion (D_{ik}^{eff}) are important, D_i^{eff} can be written as:

$$D_i^{eff} = \left(\frac{1}{D_{im}^{eff}} + \frac{1}{D_{ik}^{eff}}\right) \quad (15)$$

D_{im}^{eff} and D_{ik}^{eff} depend on the micro-structure of the porous electrode and operating conditions, the detailed calculation of these two parameters are described in .

2.2.4. Momentum conservation model

The general Navier-Stokes equation is used to describe the momentum conservation. For momentum conservation in channels, the equation can be described as:

$$\rho\frac{\partial u}{\partial t} + \rho u\nabla u = -\nabla p + \nabla\left[\mu\left(\nabla u + (\nabla u)^T\right) - \frac{2}{3}\mu\nabla u\right] \quad (16)$$

For momentum conservation in porous electrodes and anode chamber, the equation is modified by including the Darcy's term for momentum conservation in the porous layer:

$$\rho\frac{\partial u}{\partial t}+\rho u\nabla u=-\nabla p+\nabla[\mu\left(\nabla u+(\nabla u)^{T}\right)-\frac{2}{3}\mu\nabla u\Big]-\frac{\varepsilon\mu u}{k} \quad (17)$$

where ρ is the gas density, u is the velocity vector, p is pressure and ε is the porosity the electrode.

2.3. Boundary conditions

2.3.1. Electrochemical reaction

The electric potentials are specified at the outer boundaries of cathode and anode as working potential and zero potential, respectively. Insulation condition is applied to the bottom and top of the cell.

2.3.2. Mass transport

Inflow gas mole fraction is specified at cathode. The convective flux boundary condition is specified at the outlet of the cathode and anode. Zero flux is assumed at the end of anode chamber, electrolyte/electrode interface and the ends of electrodes.

2.3.4. Momentum transport

Standard gas flow rate (standard cubic centime per minute: SCCM) is specified at cathode while pressure condition is specified at the outlet. No slip condition is applied to the end of anode chamber, electrolyte/electrode interface and the ends of electrodes.

2.4. Model parameters

For model validation, the values of material property and operation parameters are consistent with experiments[13], as shown in Table 1, Table 2 and Table 3. The electrochemical characteristics of the model are validated by the experimental data using H_2 as SOFC fuel. The DC-SOFC exchange current density ($i_{0,co}$) is assumed to be 0.45 times of H_2-SOFC exchange current density ($i_{0,H2}$) as shown in experiments. The reaction rate of Boudouard reaction is affected by reaction area, activity of catalyst et al. These effects are validated by tuning the equilibrium parameter k_{rb}. The electrochemical parameters used in DC-SOFEC are the same with those validated in DC-SOFC model due to the reversible characteristic of cell. The tuning parameters used for base-case simulation are summarized in Table 4. In parametric studies, those parameters are varied to evaluate their effects on the DC-SOFEC performance.

2.5. Model solution

The model is solved by setting a certain cell voltage/inlet gas flow rate/temperature. The outputs of the model are the distributions of current density, species concentration, chemical reaction rates and others. The calculations are performed using the finite element commercial software COMSOL MULTIPHSICS®.

3. Results and discussion

3.1. Model validation

In this section, the modeling results of current-voltage characteristics are compared with experimental data for model validation. The comparison results between simulation and experimental data are shown in Fig. 2 and good agreement between them is observed. In the subsequent parametric simulation, the same cell structure parameters and tuning parameters are used and the length of the cell is extended to 90mm to increase the utilization of cathode gas. The operation temperature, voltage, inlet gas flow rate and the distance between carbon chamber and anode electrode (D_{ce}) are varied to study their effects on DC-SOFEC performance.

3.2. Effect of applied voltage

The effects of operating voltage on DC-SOFEC electrolysis of H_2O and its detailed operation conditions are shown in Fig. 3 and Table 5, respectively.

It is found that the DC-SOFEC is capable of electrolyzing H_2O and producing electrical power simultaneously when the current density is less than 3000A/m^2. When the current density for electrolysis is higher than 3000A/m^2, the operating voltage becomes negative and the cell is consuming electrical power.

Compared with conventional SOEC, DC-SOFEC electrolysis not only operates at a much lower voltage, but also realizes gas-electricity co-generation, consistent with experimental observation[13]. The co-generation is very attractive and enables SOEC to consume carbon for H_2 production at a high efficiency and a low cost.

It is also found that the molar fraction of CO in anode output gas (Fig.4) is very high (almost close to 1) under different operating voltages. On the other side (cathode), H_2 is generated by the electrolysis of H_2O in cathode. CO and H_2 produced separately at two different electrodes of DC-SOFEC can be stored or mixed to produce syngas with any desired H_2/CO ratio, which can overcome the problem of syngas composition control in H_2O/CO_2 co-electrolysis by conventional SOEC. The easy control of syngas composition by DC-SOFEC can greatly facilitate subsequent processes of syngas for various chemical or fuel generation.

3.3. Effect of operating temperature

The effects of operating temperature on DC-SOFEC performance are shown in Fig. 5 and Fig. 6. The detailed operation conditions are shown in Table 6.

It is found that the H_2 molar fraction at the cathode outlet of DC-SOFEC increases significantly with increasing temperature at a low operating voltage such as 0.2V or 0V. However, the H_2 molar fraction only increases slightly at a higher operating voltage, i.e. 0.4V and 0.6V. This phenomenon is due to the temperature-dependence of the electrochemical/chemical reaction kinetics and the ionic conductivity. The increased temperature can increase the electrochemical reaction kinetics, ionic conductivity, and the Boudouard reaction rate. As a higher rate of Boudouard reaction can produce more CO, it can increase the anode partial equilibrium potential thus increase the current density at a given operating voltage. In addition, the concentration overpotential is very significant when the current density is high, especially when the gas concentration at the TPB is close to zero. The higher CO concentration can significantly enlarge the limiting current density, thus significantly improve the performance of DC-SOFEC at a high current density (or low operating voltage). . When the operating voltage is close to 0, the H_2 molar fraction at the cathode outlet can reach almost 100%. Under this condition, the DC-SOFEC is actually an electrochemical reactor, producing H_2 and CO at the two electrodes without generating or consuming electricity. For comparison, in the conventional chemical reactors based on reforming reaction to convert carbon or hydrocarbon fuels for syngas production, both H_2 and CO are produced in the same reactor and it is usually difficult to control the gas composition. In the proposed DC-SOFEC, it is feasible to collect pure H_2 from DC-SOFEC at a reasonably high temperature and the CO molar fraction at the anode outlet can also be kept at a high level as shown in Fig.6. The overall benefits resulted by higher temperature is a higher output current density (at a given voltage) and a higher anode outlet CO molar fraction as well. To this end, it indicates that DC-SOFEC has a great potential for electricity and syngas cogeneration at high temperature.

3.4. Effect of gas flow rate at the cathode inlet

The gas flow rate at the cathode inlet is also varied to examine its effect on DC-SOFEC electrolysis of H_2O at different applied potentials and temperature. This gas flow rate changes from 50 SCCM to 300 SCCM with different applied voltages and temperatures. More detailed operation conditions can be seen in Table. 7.

A higher flow rate of the H_2O leads to higher reactant concentration in the downstream, which helps increase the cathode partial equilibrium potential and overall cell performance. However, increasing higher cathode flow rate also brings the problem of low reactant utilization as can be seen in Fig. 7: when the cathode flow rate is small, almost 100% H_2O can be converted to H_2 at high temperature (1173K) and 0V voltage. At lower temperature and higher operating voltage, the conversion ratio of H_2O decreases quickly. Therefore, a higher temperature is favored and the cathode flow rated should be carefully considered as it is not only related with the reactant utilization but

also the extra pump work. The determination of the optimal flow rate requires a detailed thermodynamic analysis.

3.5. Effect of distance between carbon and anode electrode

Since the source of CO for electricity generation is the Boudouard reaction between carbon (from carbon chamber) and CO_2 (from electrochemical reaction in anode electrode), the transport of CO from carbon chamber to anode TPB sites and CO_2 from TPB sites to carbon chamber is crucial to cell performance. It is expected that the distance between carbon chamber and anode electrode, noted as D_{ce}, play an important role in the transport of CO and CO_2, which is discussed in this section from the simulated results in Fig. 8 and Fig. 9. The detailed operation conditions are shown in Table 8.

As expected, the cathode outlet H_2 molar fraction of DC-SOFEC increases with decreasing D_{ce} (Fig. 8). Compared with low operating temperature, the performance of DC-SOFEC working at a high temperature has a much higher improvement with decreasing D_{ce}. This phenomenon is caused by both gas transport and electrochemical reaction rate. Besides, a higher temperature ensures a high outlet H_2 molar fraction even at larger D_{ce} conditions. As can be seen in Fig. 9, the molar fraction of CO at anode outlet is very close in different D_{ce} conditions at high temperature. When D_{ce} is very small ($D_{ce} = 59\mu m$), the CO fraction in anode electrode is very close to 1. As D_{ce} is increased, the transport of CO from carbon chamber to anode active sites (TPB) becomes more difficult. Thus, the molar fraction of CO decreases in anode active sites with the increase of D_{ce} especially at a low temperature (973K).

4 Conclusions

A multi-physics FEM model including electrochemical reactions, chemical reactions, ion/electronic charge transport, mass transport and momentum transport is developed to characterize the performance of a DC-SOFEC. The model is validated by comparing the simulation results with experimental date of Liu's group.

It is found that the performance of DC-SOFEC is highly dependent on the operating temperature. At a higher temperature, DC-SOFEC can co-generate electricity and CO simultaneously in a more efficient way. For comparison, the performance of DC-SOFEC is greatly reduced at a low temperature due to the low Boudouard reaction rate. Compared with conventional H_2O/CO_2 co-electrolysis for syngas production, DC-SOFEC is advantageous as H_2 and CO are produced at two different electrodes. The separate generation of H_2 and CO allows easy control of syngas composition, which is critical for subsequent chemical or fuel production.

It is also found that the performance of DC-SOFEC is largely affected by the distance between carbon chamber and anode electrode D_{ce}. With the increase of D_{ce}, the performance of DC-SOFEC decreases, demonstrating that a smaller D_{ce} is recommended in the design of DC-SOFEC in real applications for co-generation. Another point that should be noted is the choice of cathode inlet gas flow rate by considering the reactant utilization and pump work.

Acknowledgement

This research is supported by a grant of SFC/RGC Joint Research Scheme (X-PolyU/501/14) from Research Grant Council, University Grants Committee, Hong Kong SAR.

Nomenclature

Abbreviation

Ag-GDC	The mixture of silver and GDC
DC-SOFC	Solid oxide fuel cell direct using carbon as fuel
DC-SOFEC	Direct carbon assisted solid oxide electrolysis cell
GDC	Gadolinium doped ceria, $Ce_{0.8}Gd_{0.2}O_{1.9}$
GD-DCFC	Gasification driven direct carbon fuel cell
H_2-SOFC	Solid oxide fuel cell using H_2 as fuel
PEN	Positive Electrode-Electrolyte-Negative electrode assembly
SCCM	Standard cubic centime per minute
SOEC	Solid oxide electrolysis cell
SOFC	Solid oxide fuel cell
TPB	Triple phase boundary
YSZ	Yttrium stabilized zirconium

Roman

D_{ce}	Distance between carbon and anode electrode
D_i^{eff}	Effective diffusivity of species i, $m^2 \cdot s^{-1}$
D_{ik}^{eff}	Knudsen diffusion coefficient of i, $m^2 \cdot s^{-1}$
D_{im}^{eff}	Molecular diffusion coefficient of i, $m^2 \cdot s^{-1}$
E	Equilibrium Nernst potential, V
E_a	Active energy, $J \cdot mol^{-1}$
F	Faraday constant, 96485 $C \cdot mol^{-1}$
i_o	Exchange current density, $A \cdot m^{-2}$
k	Reaction rate constant, in terms of m, mol, Pa and s
K_{br}	Equilibrium constant of Boudouard reaction
L_{cell}	Length of the cell, mm
n	Number of electrons transferred per electrochemical reaction
N_i	Flux of mass transport, $kg \cdot m^{-3} \cdot s^{-1}$
p	(partial) Pressure, Pa
R	Gas constant, 8.314 $J \cdot mol^{-1} \cdot K^{-1}$
R_{ce}	Ratio D_{ce} and cell length
T	Temperature, K
u	Velocity field, $m^3 \cdot s^{-1}$
v	Volume fraction

Greek letters

α	Charge transfer coefficient
β_{H_2}	Electrochemical kinetics parameter for H_2
ε	Porosity
κ	Permeability, m^2
$\emptyset$	Potential, V
ρ	Fluid density, $kg \cdot m^{-3}$
τ	Tortuosity
μ	Dynamic viscosity of fluid, Pa·s
η_{act}	Anode activation polarization, V
η_{ohmic}	Ohmic polarization, V

Subscripts

an	Anode
ca	Cathode
l	Ionic phase
s	Electronic phase
co	Carbon monoxide

Superscripts

0	Parameter at equilibrium conditions
eff	Effective
L	Local

References

1. J. Martinez-Frias, A.-Q. Pham, and S. M. Aceves, Int J Hydrogen Energ, 28 (5), 483-490 (2003).
2. W. Wang, J. M. Vohs, and R. J. Gorte, Topics in Catalysis, 46 (3), 380-385 (2007).
3. G. Tao, B. Butler, and A. Virkar, ECS Transactions, 35 (1), 2929-2939 (2011).
4. Y. Luo, Y. Shi, W. Li, M. Ni, and N. Cai, Int J Hydrogen Energ, 39 (20), 10359-10373 (2014).
5. S. Gopalan, G. Ye, and U. B. Pal, J Power Sources, 162 (1), 74-80 (2006).
6. B. Ewan and O. Adeniyi, Energies, 6 (3), 1657 (2013).
7. A. C. Lee, R. E. Mitchell, and T. M. Gür, J Power Sources, 194 (2), 774-785 (2009).
8. Y. Xie, Y. Tang, and J. Liu, Journal of Solid State Electrochemistry, 17 (1), 121-127 (2012).
9. B. R. Alexander, R. E. Mitchell, and T. M. Gür, J Electrochem Soc, 159 (12), F810-F818 (2012).
10. Y. Bai, Y. Liu, Y. Tang, Y. Xie, and J. Liu, Int J Hydrogen Energ, 36 (15), 9189-9194 (2011).
11. B. R. Alexander, R. E. Mitchell, and T. M. Gür, J Power Sources, 228 132-140 (2013).
12. D. U. Johnson, R. E. Mitchell, and T. M. Gür, ECS Transactions, 61 (1), 235-243 (2014).
13. Y. Xie, W. Cai, J. Xiao, Y. Tang, J. Liu, and M. Liu, J Power Sources, 277 1-8 (2015).
14. E. Mon and N. R. Amundson, Industrial & Engineering Chemistry Fundamentals, 17 (4), 313-321 (1978).

Tables

Table.1 Model parameters

Parameters	**Value or expression**	**Unit**
Ionic conductivity		
GDC	$\frac{100}{T} \times 10^{(6.66071\ -\ \frac{5322.92}{T})}$	Sm^{-1}
YSZ	$3.34 \times 10^4 e^{\frac{-10300}{T}}$	Sm^{-1}
Electronic conductivity		
Ag	$\frac{1.59e^8}{(0.0038T-0.1134\ 丿)}$	Sm^{-1}
Porosity		
Cathode	0.46	
Anode	0.46	
Electrode volume fraction		
GDC	0.21	
Ag	0.79	
S_{TPB}		
Cathode layer	2.14×10^5	m^2m^{-3}
Anode layer	2.14×10^5	m^2m^{-3}

Table. 2 Operation parameters for model validation (H_2-SOFC)

Parameter	**Value**	**Unit**
Anode inlet gas flow rate for	50	SCCM
Cathode inlet gas flow rate	10	SCCM
Anode inlet gas composition	H_2(97%) + H_2O(3%)	
Cathode inlet gas composition	Air	
Temperature	1123	K

Table. 3 Operation parameters for model validation (DC-SOFC)

Parameter	**Value**	**Unit**
Distance between anode chamber and electrode, D_{ce}	**59**	**μm**
Cathode inlet gas flow rate	10	SCCM
Cathode gas composition	Air	
Temperature	1123	K

Table.4 Model tuning parameters

Parameter	**Value**	**Unit**
Cathode tortuosity	3	
Anode tortuosity	3	
H_2 exchange current density, i_{H_2}	1000	Am^{-2}
O_2 exchange current density i_{O_2}	400	Am^{-2}
CO exchange current density, i_{CO}	450	Am^{-2}
H_2 charge transfer coefficient, α_{H_2}	0.5	
CO charge transfer coefficient, α_{CO}	0.5	
O_2 charge transfer coefficient, α_{O_2}	0.5	
Equilibrium constant of Boudouard reaction	6×10^{13}	1/s

Table. 5 Operation parameters for operating potential effect study in DC-SOFC

Parameter	**Value**	**Unit**
Operating voltage	-0.1 – 0.7	V
Cathode inlet gas flow rate	100	SCCM
Cathode gas composition	H_2O	
Temperature	1123	K

Table. 6 Operation parameters for temperature effect study in DC-SOFC

Parameter	**Value**	**Unit**
Operating voltage	0, 0.2, 0.4, 0.6	V
Cathode inlet gas flow rate	100	SCCM
Cathode gas composition	H_2O	
Temperature	973 - 1203	K

Table. 7 Operation parameters for inlet H_2O flow rate effect study in DC-SOFC

Parameter	**Value**	**Unit**
Operating voltage	0, 0.2	V
Cathode inlet gas flow rate	50 - 300	SCCM
Cathode gas composition	H_2O	
Temperature	1073, 1173	K

Table. 8 Operation parameters for D_{ce} effect study in DC-SOFC

Parameter	**Value**	**Unit**
Operating voltage	0	V
Distance between anode chamber and electrode, D_{ce}	59 - 4559	μm
Cathode inlet gas flow rate	100	SCCM
Cathode gas composition	H_2O	
Temperature	1073 - 1273	K

Figures:

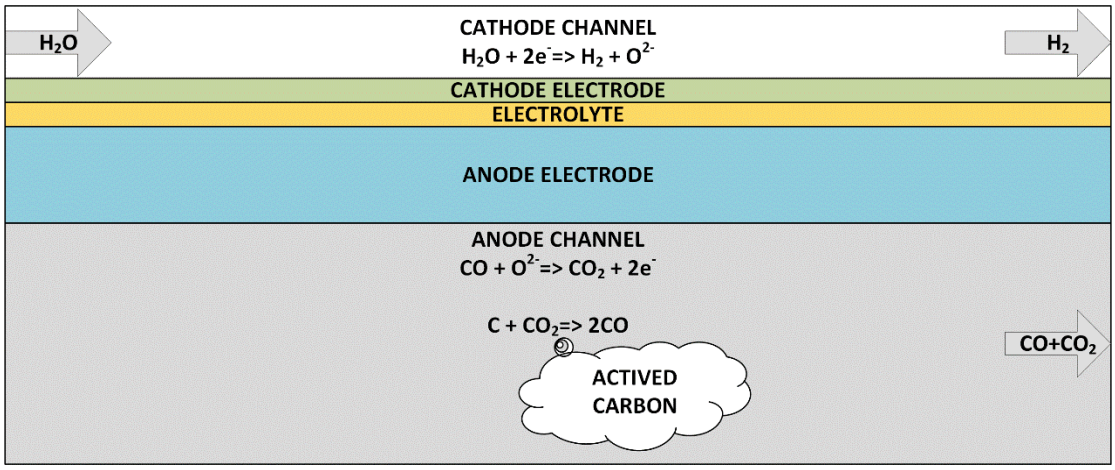

Fig.1. Schematic of DC-SOFEC

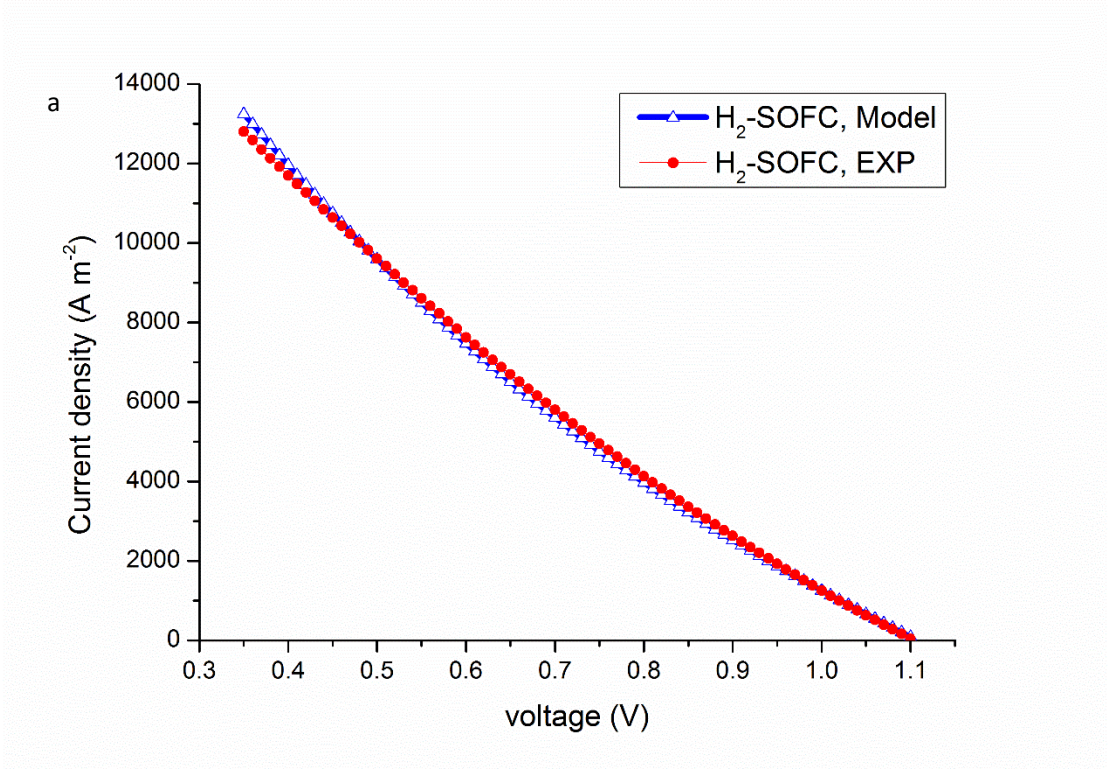

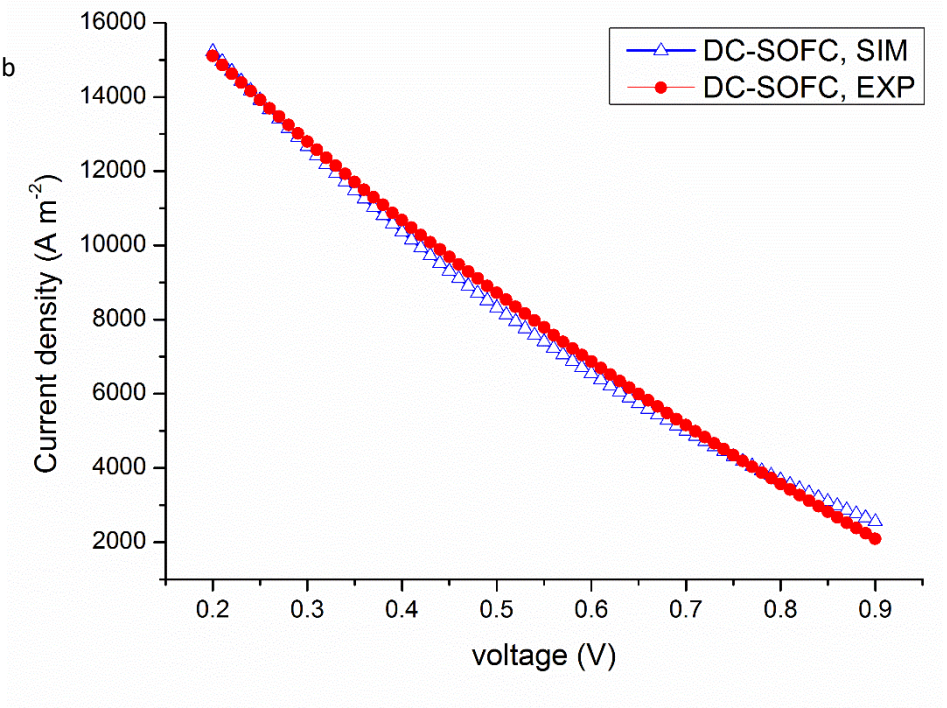

Fig.2 Model validation for (a) H_2-SOFC and (b) DC-SOFC

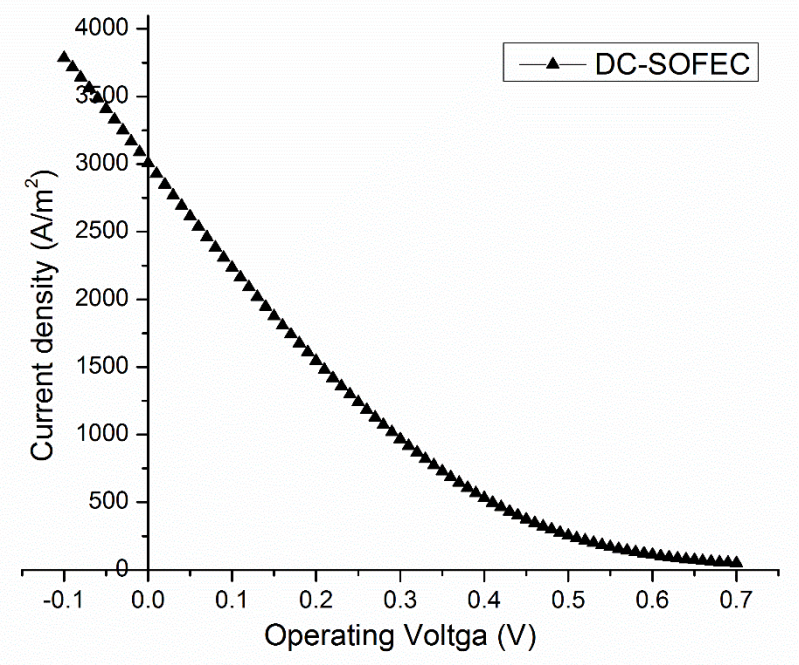

Fig.3. Effect of operating voltage on DC-SOFEC performance at 1123K

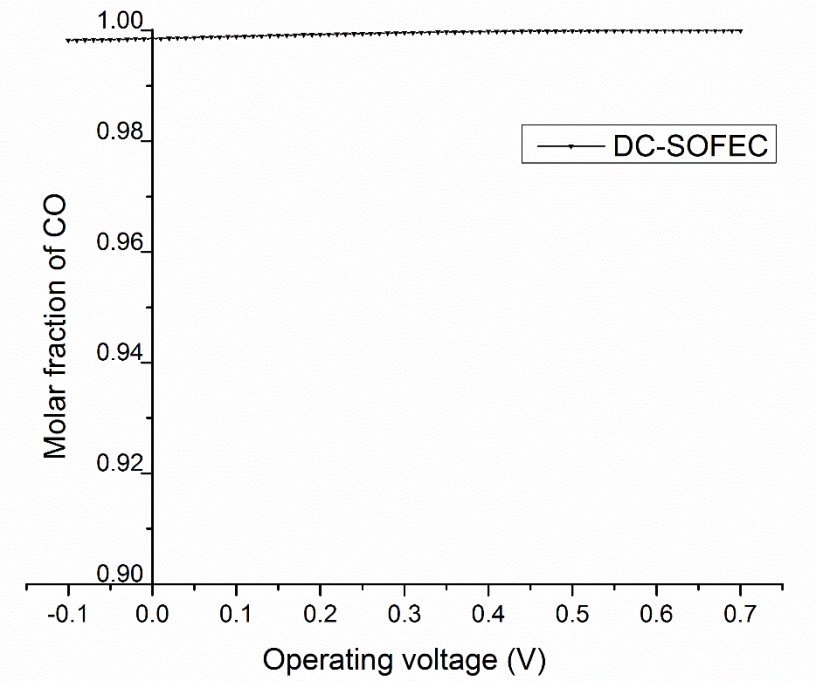

Fig.4. Effect of operating voltage on anode outlet CO molar fraction in DC-SOFEC at 1123K.

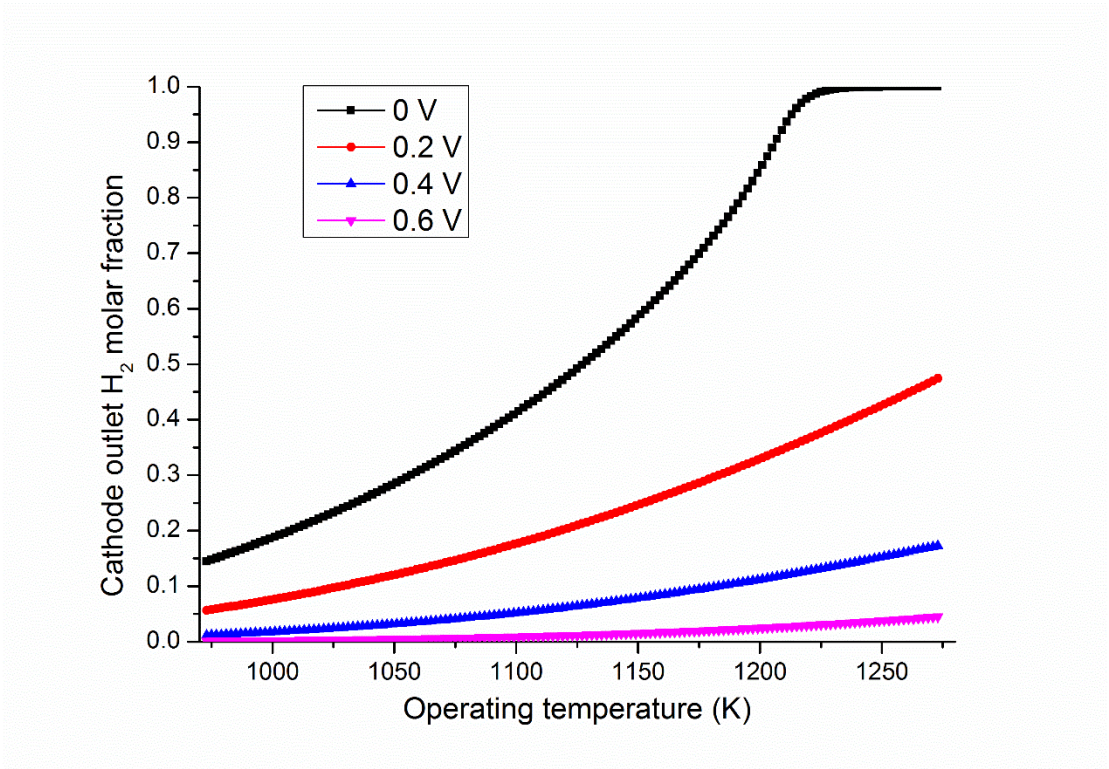

Fig.5. Effect of temperature on DC-SOFEC cathode outlet H_2 molar faction at different operating voltages.

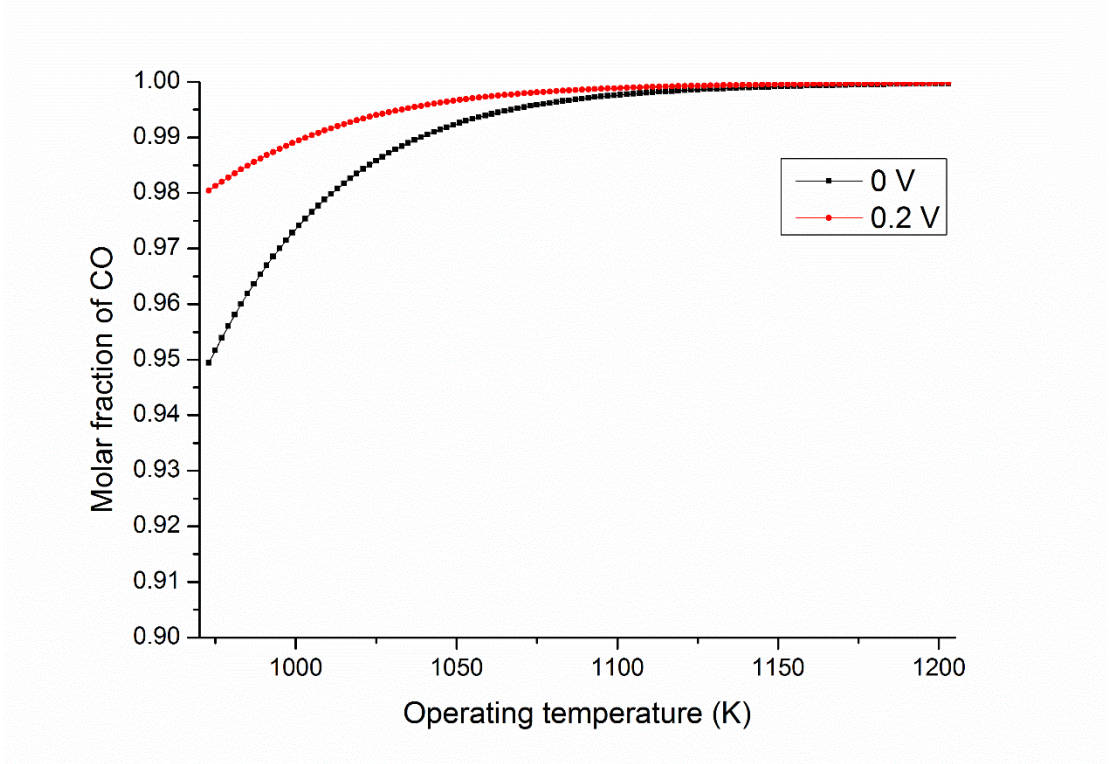

Fig.6. Effect of operating temperature on anode outlet CO molar fraction in DC-SOFEC at 0V and 0.2V operating voltages.

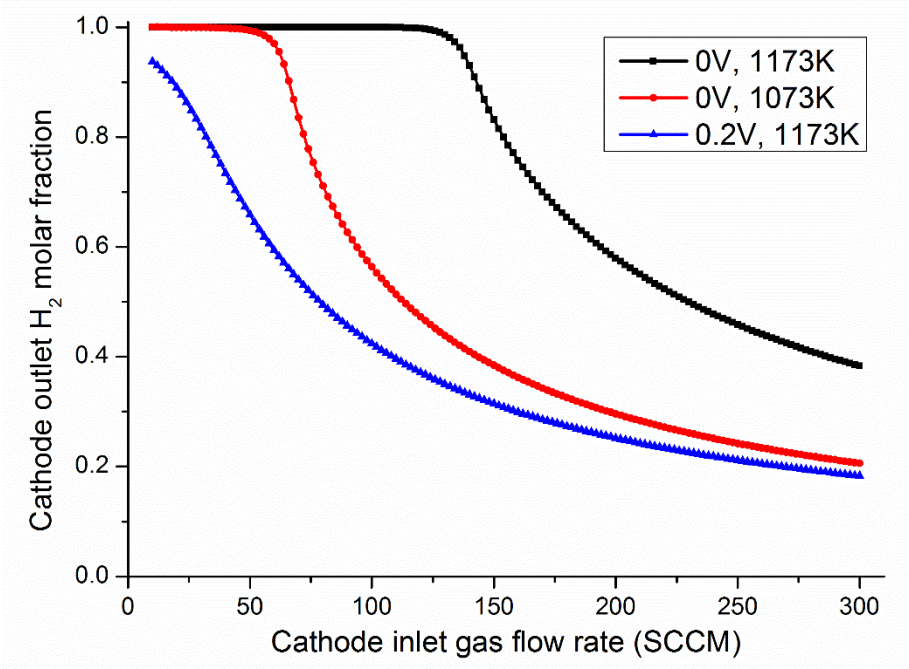

Fig.7. Effect of cathode inlet gas flow rate on outlet H_2 molar fraction at 1073K and 1173K operating temperatures and 0V and 0.2V operating voltages.

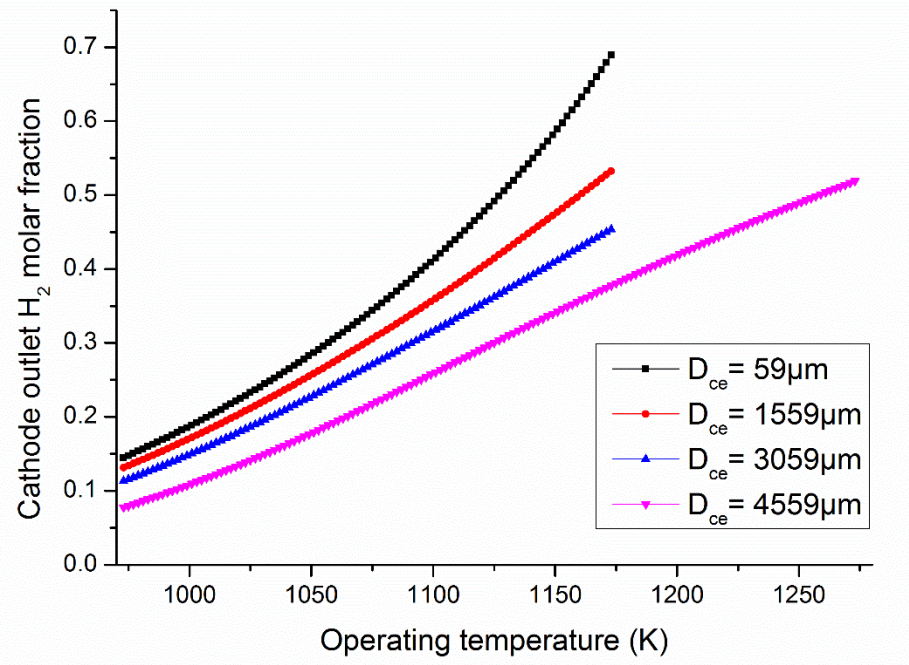

Fig.8. Effect of operating temperature on cathode outlet H_2 molar fraction at different D_{ce} situations.

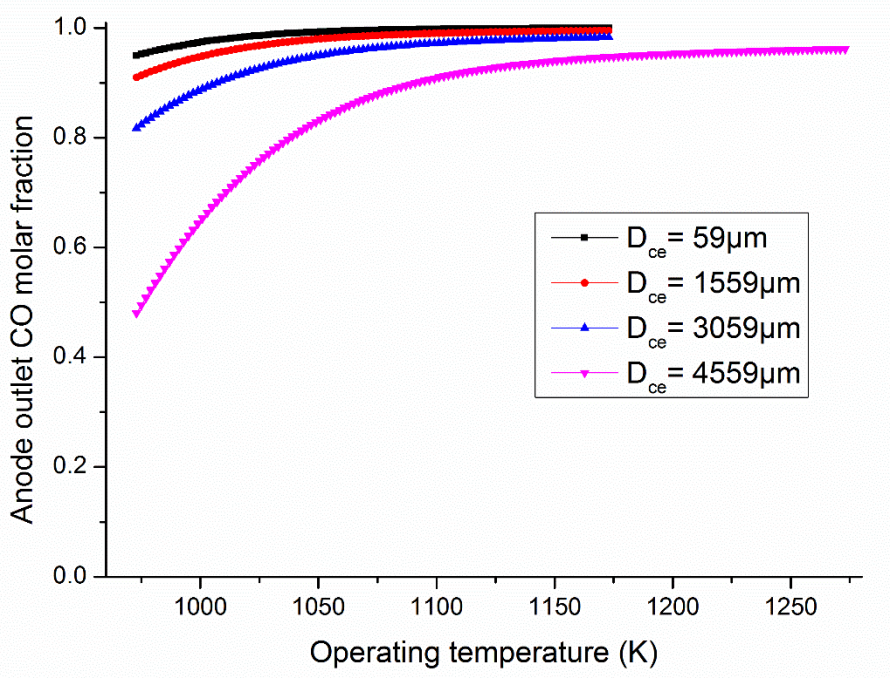

Fig.9. Effect of operating temperature on anode outlet CO molar fraction at different D_{ce} situations.